

Quantum simulation via filtered Hamiltonian engineering: application to perfect quantum transport in spin networks

Ashok Ajoy and Paola Cappellaro

*Department of Nuclear Science and Engineering and Research Laboratory of Electronics,
Massachusetts Institute of Technology, Cambridge, MA, USA*

We propose a novel Hamiltonian engineering method in spin-based quantum information processing architectures that requires no local control but only relies on collective spin rotations and field gradients. The technique relies on coupling engineering via the time-domain construction of a Bragg grating and a weighting function that modulate the coupling strengths. As an example, we demonstrate how to engineering the optimal Hamiltonian for perfect quantum information transport between two separated nodes of a large spin network. We engineer a spin chain with optimal couplings from a large spin network, such as naturally occurring in crystals, while decoupling all unwanted interactions. We show that for realistic experimental parameters this Hamiltonian engineering method could be used for perfect quantum information transport at room-temperature.

PACS numbers: 03.67.Ac, 76.60.-k, 03.67.Lx

Introduction – Controlling the evolution of complex quantum systems has emerged as an important area of research for its promising practical applications. Such control can be often reduced to the goal of Hamiltonian engineering [1] (also extended to reservoir engineering [2–4]). Hamiltonian engineering has been used to achieve a variety of tasks, including quantum computation [5], improved quantum metrology [6] and protection against decoherence by dynamical decoupling filtering [7, 8]. The most important application is quantum simulation [9], as first proposed by Feynman [10]. The ultimate goal is to achieve a programmable universal quantum simulator, able to mimic the dynamics of any system. A possible strategy is to use a quantum computer and decompose the desired evolution into unitary gates [11, 12]. Alternatively, one can use Hamiltonian engineering by a Suzuki-Trotter factorization of the desired interaction into experimentally achievable Hamiltonians [13, 14]. However, experimental implementations of these simulation methods often require local quantum control, which is difficult to achieve in large quantum systems.

Instead, here we present a general scheme for quantum simulation that employs only collective rotations of the qubits and field gradients – technology which is in everyday use e.g. in magnetic resonance imaging or in optical lattices [15]. We consider a qubit network with an internal Hamiltonian H_{int} , for example due to the dipolar coupling between spins in a crystal lattice. The target Hamiltonian is then engineered from H_{int} in two steps: First, unwanted couplings are removed (*decoupled*) by evolution under the gradient field, in a manner equivalent to the construction of a time-domain Bragg grating \mathcal{G}_{ij} [7]. The grating acts like a sharp filter, letting through only specific couplings [16]. Then, a time-domain weighting function F modulates the coupling strengths to match the target Hamiltonian.

For concreteness, we show how to apply this filtered engineering method to the specific problem of generating

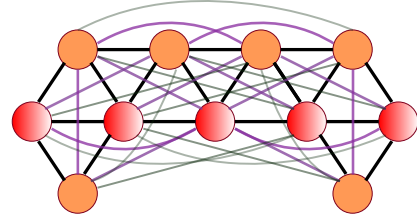


FIG. 1. A complex spin network in a trigonal planar lattice consisting of a linear chain (red) and surrounding network (orange). The edges denote couplings between the spins. A linear magnetic field gradient is aligned in the direction of the chain, such that the gradient strength at spin j is $\omega_j = j\omega$. The filter eliminates off-chain couplings as well as NNN couplings.

an optimal Hamiltonian for quantum information transfer (QIT) between two separated nodes of a spin network. Linear arrays of spins have been proposed as quantum *wires* for this task [17] and engineering the coupling between the spins can achieve perfect QIT [18]. We will finally analyze experimental requirements to implement the method in existing physical architectures.

Hamiltonian engineering – The goals of filtered Hamiltonian engineering can be summarized as (i) the cancellation of unwanted couplings – often next-nearest neighbor (NNN) and other long range couplings – and (ii) the engineering of the remaining couplings – for example, nearest neighbor (NN) couplings – to match the desired coupling strengths. We achieve these goals by dynamically generating tunable and independent grating (\mathcal{G}_{ij}) and weighting (F_{ij}) functions by means of collective rotations and gradients. The first step is to create from H_{int} the Hamiltonian operator one wishes to simulate. This can be done using sequences of collective pulses. Although the initial natural Hamiltonian restricts what operators can be obtained (see Appendix), various control sequences have been proposed to realize a broad

set of operators [19–21] starting from either the secular dipolar Hamiltonian or an Ising interaction. These multiple pulse sequences cannot however modulate the coupling strengths, which is instead our goal. Evolution under a magnetic field gradient imposes a modulation of the coupling strength. Consider for example that we want to modify the isotropic XY Hamiltonian, $H_{XY} = \sum_{ij} b_{ij}(S_i^x S_j^x + S_i^y S_j^y)$. To first order, evolution under the propagator $U(t, \tau) = e^{-iH_z \tau} e^{-H_{XY} \tau} e^{iH_z \tau}$, where $H_z = \sum_i \omega_i S_i^z$ is obtained by a gradient, is equivalent to the evolution under the effective Hamiltonian

$$H'_{XY} = \sum_{ij} b_{ij} [(S_i^x S_j^x + S_i^y S_j^y) \cos(\delta\omega_{ij}\tau) + (S_i^x S_j^y - S_i^y S_j^x) \sin(\delta\omega_{ij}\tau)],$$

where $\delta\omega_{ij} = \omega_j - \omega_i$. The modulation can then be repeated to obtain a total propagator $U_0 = \prod_h U(t_h, \tau_h)$. Given a desired target Hamiltonian $H_d = \sum_{ij} d_{ij}^1 (S_i^x S_j^x + S_i^y S_j^y) + d_{ij}^2 (S_i^x S_j^y - S_i^y S_j^x)$, we thus obtain a set of equations in the unknowns $\{t_h, \tau_h\}$ that allow Hamiltonian engineering. To simplify the search for the correct timings, we can further apply a filter that cancels all unwanted couplings and use the equations above to only find the remaining, non-zero coupling strength. The filter is obtained by creating a dynamic *grating*: instead of the propagator U_0 , we evolve under N cycles (while reducing the times $t_h \rightarrow t_h/N$) with a gradient modulation $U = \prod_{k=1}^N e^{-iH_z \tau^k} U_0 e^{iH_z \tau^k}$, which imposes a weighting factor \mathcal{G}_{ij} to the couplings, analogous to a dynamical implementation of a Bragg grating [7],

$$\mathcal{G}_{ij} = \sum_{k=0}^{N-1} e^{ik\tau\delta\omega_{ij}} = e^{i(N-1)\tau\delta\omega_{ij}/2} \frac{\sin(N\tau\delta\omega_{ij}/2)}{\sin(\tau\delta\omega_{ij}/2)}.$$

We now make these ideas more concrete by considering a specific example, the engineering of an Hamiltonian allowing perfect QIT in mixed-state spin chains, thus enabling room temperature quantum communication [21–26]. For lossless transport, the simplest engineered n -spin chain consists of only NN couplings that vary parabolically along the chain, $d_j = d\sqrt{j(n-j)}$ [18, 27]. This ensures perfect transport in a time $T = \pi/(2d)$. However, manufacturing chains with such restricted coupling topologies is a hard engineering challenge due to fabrication constraints and the intrinsic presence of long-range interactions [28, 29]. On the other hand, *regular*, lattice-based spin networks (see e.g. Fig. 1) are found ubiquitously in nature. Our method can then be used to dynamically engineer the optimal Hamiltonian starting from a complex spin network.

Filtered engineering for QIT – The target Hamiltonian for QIT in a n -spin chain is $H_d = \sum_{j=1}^{n-1} d_j (S_j^x S_{j+1}^x - S_j^y S_{j+1}^y)$. We consider a dipolarly coupled spin network with Hamiltonian

$$\mathcal{H} = \mathcal{H}_{\text{int}} + \mathcal{H}_z = \sum_{ij} b_{ij} (3S_i^z S_j^z - S_i \cdot S_j) + \sum_i \omega_i S_i^z, \quad (1)$$

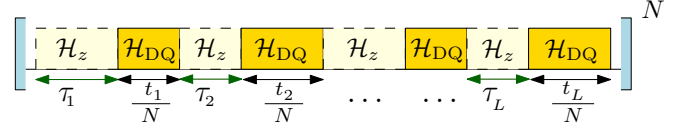


FIG. 2. The filtered engineering control sequence consists of alternating blocks of evolution under the gradient \mathcal{H}_z for times τ_j and DQ evolution \mathcal{H}_{DQ} of duration t_j/N . The fundamental cycle is repeated N times.

where the spatial *tagging* of the frequencies is achieved by applying an appropriate magnetic field gradient. The double-quantum Hamiltonian $\mathcal{H}_{\text{DQ}} = \sum_{i<j} b_{ij} (S_i^x S_j^x - S_i^y S_j^y)$ can be obtained from the secular dipolar Hamiltonian via a well-known multiple-pulse sequence [19], which at the same time cancels the term \mathcal{H}_z . Importantly, the sequence allows time-reversal of the evolution by a simple phase shift of the pulses. We can further impose evolution under the field gradient only, \mathcal{H}_z , by using homonuclear decoupling sequences, such as WAHUA [30, 31] or magic echo trains [32]. Alternatively, homonuclear decoupling can be avoided by shifting the DQ sequence off-resonance during the free evolution period (see Appendix).

A control sequence achieving filtered Hamiltonian engineering consists of alternating blocks of evolution under \mathcal{H}_z and double quantum excitation \mathcal{H}_{DQ} (*mixing* period, see Fig. 2). We analyze the net effect of this pulse sequence using average Hamiltonian theory [31]. Let us consider for simplicity a sequence with only two mixing and free evolution blocks. Then setting $U_z(\tau) = \exp(-i\tau\mathcal{H}_z)$ and $U_{\text{DQ}}(t) = \exp(-it\mathcal{H}_{\text{DQ}})$, the propagator corresponding to N cycles is, $U_N = [U_z(\tau_1)U_{\text{DQ}}(\frac{t_1}{N})U_z(\tau_2)U_{\text{DQ}}(\frac{t_2}{N})]^N$, which can be rewritten as,

$$U_N = [U_z(\tau_1)U_{\text{DQ}}(\frac{t_1}{N})U_z^\dagger(\tau_1)] \times [U_z(\tau_1 + \tau_2)U_{\text{DQ}}(\frac{t_2}{N})U_z^\dagger(\tau_1 + \tau_2)] \times \cdots \times [U_z((N-1)\tau)U_{\text{DQ}}(\frac{t_2}{N})U_z^\dagger((N-1)\tau)] \quad (2)$$

where $\tau = \tau_1 + \tau_2$. Now, $[U_z(\tau_1)U_{\text{DQ}}(\frac{t_1}{N})U_z^\dagger(\tau_1)] = \exp(-i\frac{t_1}{N}H_m(\tau_1))$, where $H_m(\tau_1) = \sum_{i<j} b_{ij} (S_i^+ S_j^+ e^{i\tau_1\delta_{ij}} + S_i^- S_j^- e^{-i\tau_1\delta_{ij}})$ is the *tagging* frame Hamiltonian with $\delta_{ij} = \omega_i + \omega_j$. Employing the Suzuki-Trotter approximation [14], the propagator U_N is equivalent to evolution under the average Hamiltonian,

$$\bar{H} = \sum_{i<j} \frac{b_{ij}}{N} S_i^+ S_j^+ \left(t_1 e^{i\tau_1\delta_{ij}} + t_2 e^{i(\tau_1+\tau_2)\delta_{ij}} \right) \mathcal{G}_{ij} + \text{h.c.}$$

where $\mathcal{G}_{ij} = e^{i(N-1)\tau\delta_{ij}/2} \frac{\sin(N\tau\delta_{ij}/2)}{\sin(\tau\delta_{ij}/2)}$ is the dynamical Bragg grating.

In general, for a sequence consisting of free periods $\tau_{\mathbf{z}} = \{\tau_1, \dots, \tau_L\}$ and mixing periods $\mathbf{t}_{\mathbf{m}} = \{t_1, \dots, t_L\}$, the average Hamiltonian is $\bar{H} =$

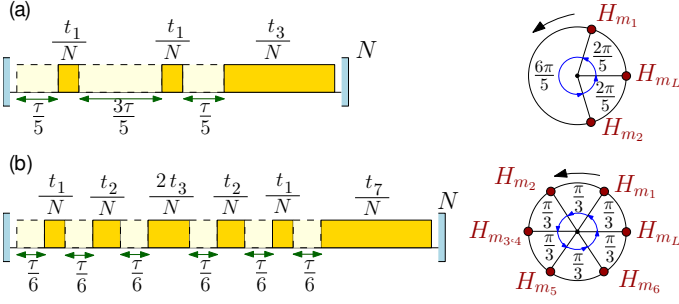


FIG. 3. Left panels show control sequences for filtered engineering in a (a) 5 spin chain and (b) a 6 spin chain. The explicit values of \mathbf{t}_m are in . In the right panels, the phase acquired by the $S_1^+ S_2^+$ term of the toggling frame Hamiltonians H_{m_j} (arising after each of the L mixing periods) is depicted on a unit circle [35]. To retain the DQ form of the average Hamiltonian, the phases have reflection symmetry about 2π (see also).

$\sum_{i < j} S_i^+ S_j^+ F_{ij}(\tau_{\mathbf{z}}, \mathbf{t}_m) \mathcal{G}_{ij}(\tau) + \text{h.c.}$ where $\tau = \sum_{j=1}^L \tau_j$ and we define the *weighting function* [7, 33],

$$F_{ij}(\tau_{\mathbf{z}}, \mathbf{t}_m) = \frac{b_{ij}}{N} \sum_k t_k \exp\left(i\delta_{ij} \sum_{h=1}^k \tau_h\right) \quad (3)$$

The grating \mathcal{G}_{ij} forms a sharp filter [7, 34] with maxima at $\tau\delta_{ij} = 2m\pi$. We assume to apply a linear 1D-magnetic field gradient along a selected chain of spins in the larger network, such that the frequency of spin j is $\omega_j = j\omega - \omega_0$, where ω_0 is the excitation frequency. Each spin pair term of the DQ Hamiltonian acquires a spatial phase tag under the gradient field: if $\omega\tau = \pi$ and $2\omega_0\tau = 3\pi - 2m\pi$ the NN couplings are preserved, while the NNN couplings lie at the minima of the grating, and are decoupled (see Fig. 4). Other non-NN, off-chain couplings (see Fig. 1), lie at the grating side-lobes, and have greatly reduced amplitudes for large N , falling off linearly with N (see Appendix). Note that a suitable choice of gradient and free evolution could impose similar phase tags to other mixing Hamiltonians – for example, through a quadratic gradient for the isotropic XY Hamiltonian.

Following the filter, the weighting function $F_{j(j+1)}$ can be constructed to yield the ideal coupling strengths required for perfect transport. Given the toggling frame Hamiltonians, $H_m(\tau_k)$, we have a set of $2n$ equations (for an n -spin chain),

$$\begin{aligned} \sum_{h=1}^L \sin(\omega(2i+1)\tau_h) t_h b_{i,i+1} &= 0, & \forall i \\ \sum_{h=1}^L \cos(\omega(2i+1)\tau_h) t_h b_{i,i+1} &\propto d_i, & \forall i, \end{aligned} \quad (4)$$

with $2L$ unknowns for L time steps. The number of conditions (and thus of time steps) can be reduced by exploiting symmetry properties. For example, by imposing a gradient symmetric with respect to the center of the chain, it could be possible to automatically satisfy most of the conditions in Eq. 4 and only $L = \lceil n/2 \rceil$ time steps

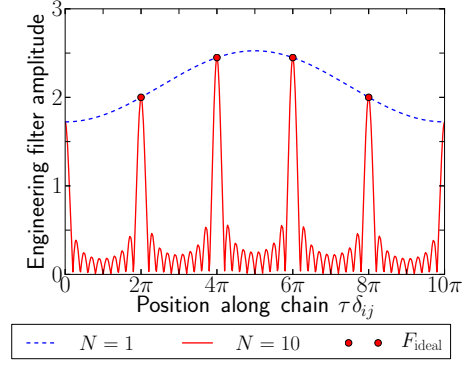


FIG. 4. Engineering filter amplitude $|F_{ij}\mathcal{G}_{ij}|$ for a 5-spin chain after different cycle numbers N . A single cycle creates the weighting function F_{ij} shown in blue, which is transformed to sharp peaks at the ideal engineered couplings (red circles) as the number of cycles increases.

would be required. Unfortunately this solution is practical only for some chain lengths (see Appendix); we thus focus on a suboptimal but simpler solution. Let us first determine $\tau_{\mathbf{z}}$ and \mathbf{t}_m for an odd n -spin chain. To enforce the mirror symmetry of the couplings d_j [36] and ensure that the average Hamiltonian remains in DQ form, we impose mirror symmetry to the times, $t_j = t_{L-j}$, while the gradient evolution intervals are $\tau_j/\tau = 3/n$ for $j = (L+1)/2$ and $\tau_j/\tau = 1/n$ otherwise (see Fig. 3). This choice yields a simple *linear* system of equations for $L = n-2$ mixing periods \mathbf{t}_m ,

$$F_{j(j+1)} \mathcal{G}_{j(j+1)} = \sum_k t_k \cos\left(\frac{2j\pi k}{n}\right) = d\sqrt{j(n-j)}$$

An intuitive phasor representation [35] of how the evolution periods exploit the symmetries involved is presented in Fig. 3 and in the Appendix. For even spin chains, the solution can be derived analogously with $L = n+1$, $t_L = \frac{1}{n-1} \sum_j d_j$ and $\tau_j = 0$ for $j = L/2 + 1$, and $\tau_{z_j}/\tau = 1/n$ otherwise.

When applied to a n -spin linear chain, the tuning action of $F_{j(j+1)} \mathcal{G}_{j(j+1)}$ is remarkably rapid, achieving perfect transport fidelity in just a few cycles (Fig. 5). Increasing the number of cycles reduces the error in the Trotter expansion improving $F_{j(j+1)}$ (as shown in Fig. 5.a) as well as improving the filter selectivity $\mathcal{G}_{j(j+1)}$ (see Fig. 5.b). In general, the peak width of the Bragg grating decreases with the number of cycles as $2\pi/N$ [7], improving the grating selectivity linearly with N (see Appendix). Indeed, if all couplings are included, about n cycles are required for almost perfect decoupling of the unwanted interactions (fidelity > 0.95 in Fig. 5).

The highly selective grating also avoids the need for the chain to be isolated and for the surrounding network to have a regular structure. Any spin that lies in between two nearest-neighbors of the chain can be ef-

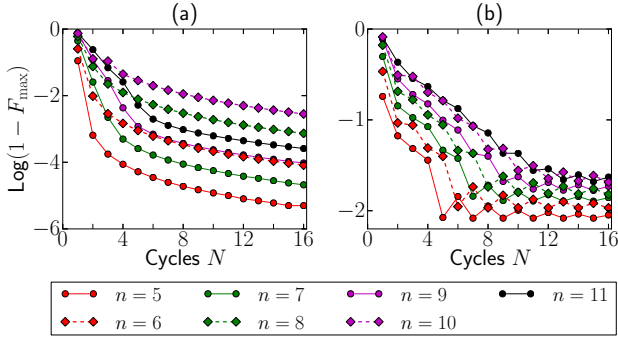


FIG. 5. Minimum transport infidelity, with filtered engineering as a function of cycle number N for a n -spin dipolar chain with (a) NN couplings only and (b) all couplings included. Here we calculated the fidelity $F = \text{Tr} \{ U S_i^z U^\dagger S_n^z \} / 2^n$. Almost perfect fidelity is achieved even for long chains with just a few filter cycles.

fectively decoupled, as shown in Fig. 6, where as small as $N = 20$ cycles are sufficient for robust QIT. However, in the presence of disorder in the couplings of the chain spins one needs to compromise between broader grating peaks (via small N) and poorer decoupling of unwanted interactions.

Approximation mechanism – The control sequence is designed to engineer only the first order average Hamiltonian \bar{H} in Eq. (3). Higher order terms contribute with errors scaling as $\mathcal{O}(t_k t_{k+1} / N^2)$, as arising from the Trotter expansion [13, 14]. Consider for example the propagator for a 5-spin chain,

$$U_N = [e^{-i \frac{t_1}{N} H_m(\tau_1)} e^{-i \frac{t_1}{N} H_m(\tau_2)} e^{-i \frac{t_L}{N} \mathcal{H}_{\text{DQ}}}]^N, \quad (5)$$

where $\tau_1 = \pi/(5\omega)$ and $\tau_2 = 2\pi/(5\omega)$ (Fig. 3). This yields the desired average Hamiltonian \bar{H} with an error $\mathcal{O}(t_1^2/N^2)$ for the first product, and $\mathcal{O}(2t_1 t_L/N^2)$ for the second. Increasing N improves the approximation, at the expense of larger overhead times (Fig. 5). In addition, the chosen scheme achieves remarkably good fidelities even for small N , since by construction, $t_j \ll t_L \approx T/N$. In essence, the system evolves under the unmodulated DQ Hamiltonian during t_L , yielding the *average* coupling strength, while the t_j periods apply small corrections required to reach the ideal couplings.

Symmetrizing the recoupling sequence would lead to a more accurate average Hamiltonian because of vanishing higher orders [14, 37]. However, this comes at the cost of larger free evolution times τ_z and a larger number of periods of the unsymmetrized sequence could be fit into this overhead time.

Experimental viability – We now consider the feasibility of experimentally implementing the filtered engineering sequence and show that high fidelity quantum transport at room temperature would be possible with current technology.

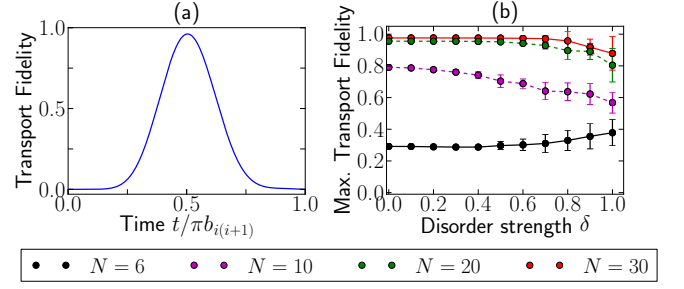


FIG. 6. (a) Transport fidelity of polarization in the network of Fig. 1 as a function of mixing time for $N = 30$. Almost perfect fidelity is reached for $t = \pi/2b_{i(i+1)}$. (b) Variation of maximum fidelity with disorder in the surrounding network. The spins of the surrounding network are displaced by $\delta \cdot r$, where δ is the disorder strength, r is a random number in $[-x/2, x/2]$ with x being the separation between NN chain spins, and we consider 30 random manifestations of the network. The filter improves as the number of cycles is increased.

For simplicity we assume that the spin chain or network is constructed in a physical lattice of NN separation r_0 , leading to a NN coupling strength $b = \frac{\mu_0 \hbar \gamma^2}{4\pi r_0^3}$. If an ideal n -spin chain can be fabricated in this lattice with maximum coupling strength b , the transport time required would be $T_{\text{id}} = \frac{n\pi}{8b}$ [22]. Alternatively, perfect state transfer could be ensured in the weak-coupling regime [21, 38–40], with a transport time $T_{\text{weak}} = \frac{\Gamma\pi}{b}$, where $\Gamma \gg 1$ ensures that the end-spins are weakly coupled to the bulk-spins. We compare T_{id} and T_{weak} to the time required for N cycles of the engineering sequence, T_{eng} . Since $t_L \gg t_j$, to a good approximation the total mixing time is $Nt_L \lesssim \sum_j \sqrt{j(n-j)}/n \approx \pi n/8$. Since $\tau = \pi/\omega$, we have

$$T_{\text{eng}} = \frac{n\pi^2}{16b} + \frac{N\pi}{\omega} \quad (6)$$

The overhead time $\frac{N\pi}{\omega}$ depends on the available gradient strength ω . Since we can take $\Gamma \approx n$ for the weak regime [21] and $N \approx n$ for filtered engineering, a gradient larger than the NN dipolar coupling strength b would allow for faster transport in the latter case. As noted above, the chosen solution is not time-optimal and further speed-ups could be obtained for particular chain lengths.

For concreteness, let us consider the crystal lattice of calcium Fluorapatite (Fap) $[\text{Ca}_5(\text{PO}_4)_3\text{F}]$ [41, 42] that has been studied for quantum transport [43, 44]. It consists of ^{19}F nuclei that form linear chains along the c -axis, each surrounded by 6 other chains. The intra-nuclear spacing within a single chain is $r_0 = 0.3442\text{nm}$, which corresponds to $b = 1.289\text{kHz}$, while the inter-chain coupling is about 40 times weaker. Gradient strengths of comparable magnitude can be made by Maxwell field coils [45]: for instance, Ref. [46] demonstrated gradient strengths of $5.588 \times 10^8 \text{G/m}$ over a 1mm^3 region; this cor-

responds to $\omega = 0.7705\text{kHz}$. Far stronger gradients are routinely used in magnetic resonance force microscopy (MRFM) [47]; for instance, dysprosium-based magnetic tips [48] yield gradients of 60G/nm , linear over distances exceeding 30nm , corresponding to $\omega = 82.73\text{kHz}$. Conservatively, one could estimate $\omega = 25\text{kHz}$, for which usual NMR $\pi/2$ -pulse widths of about $0.5\mu\text{s}$, would allow sufficient bandwidth for coherent control on chains exceeding $n = 50$ spins. In order to ensure that the experimental time does not exceed the decoherence time of the sample, one could apply homonuclear decoupling [31, 32] in the free evolution periods to reduce the effective line width by at least an order of magnitude. For FAp, evolution under the DQ Hamiltonian survives for about 1.5ms [49] as limited by pulse errors; we anticipate that decoupling during the U_z periods could increase this easily to 15ms [7, 32]. With $\omega = 25\text{kHz}$, and $N = 30$ cycles, nearly lossless transport should be possible for a 25-spin chain. Note that in this case the free evolution period per cycle is $125\mu\text{s}$, allowing at least a few cycles of WAHUA decoupling per U_z evolution.

Conclusion – We have described a method for quantum simulation without any local control, relying on the construction of time domain filter and weighting functions via evolution under a gradient field. The method was applied to engineer spin chains for perfect transport, isolating them from a large complicated networks. We showed that robust and high fidelity quantum transport can be driven in these engineered networks, with only experimental feasible control.

Appendix

Operator engineering

Nuclear Magnetic Resonance has a long tradition of control sequences able to modify the naturally occurring Hamiltonians into desired operators; the most prominent application is in the refocusing of unwanted interactions, which has been further developed and is now a common technique in quantum information under the name of dynamical decoupling. Here we extend these decoupling sequences to more general two-body Hamiltonians as well as to the task of creating a desired operator.

We consider general Hamiltonian for 2 spin- $\frac{1}{2}$:

$$H = \vec{\omega}_1 \cdot \vec{\sigma}_1 + \vec{\omega}_1 \cdot \vec{\sigma}_1 + \vec{\sigma}_1 \cdot \mathbf{d} \cdot \vec{\sigma}_2, \quad (7)$$

which can be rewritten in terms of spherical tensors $T_{l,m}$ (see Table I):

$$H = \sum_{l,m} (-1)^m A_{l,-m} T_{l,m} \quad (8)$$

where the coefficients $A_{l,-m}$ depend on the type of spin-spin interaction and the external field. This notation

is useful when considering rotations of the Hamiltonian. We consider only collective rotations –as easily achievable experimentally– that conserve the rank l .

The goal of Hamiltonian engineering by multiple pulse sequence is to obtain a desired Hamiltonian from the naturally occurring one by piece-wise constant evolution under rotated versions of the natural Hamiltonian. We thus want to impose

$$\sum_k R_k \mathcal{H}_{nat} R_k^\dagger = \mathcal{H}_{des}, \quad (9)$$

where R_k are collective rotations of all the spins, which achieves the desired operator to first order in a Trotter expansion. Rotations can be described by the Wigner matrices $D_{m,n}^l(R_k)$ as:

$$R_k T_{l,m} R_k^\dagger = \sum_{m,n} (-1)^m D_{m,n}^l(R_k) T_{l,n} \quad (10)$$

thus Eq. (9) can be written using the spherical tensors as

$$\sum_{k,n} \sum_{l,m} (-1)^m A_{l,-m}^{nat} D_{m,n}^l(R_k) T_{l,n} = \sum_{l,m} (-1)^m A_{l,-m}^{des} T_{l,m} \quad (11)$$

We thus obtain the set of equations

$$\sum_{k,m} (-1)^m A_{l,-m}^{nat} D_{m,n}^l(R_k) = (-1)^n A_{l,-n}^{des}. \quad (12)$$

We note that since collective pulses cannot change the rank l , there are limitations to which Hamiltonians can be engineered. In particular, T_{00} commutes with collective rotations: its contribution is thus a constant of the motion and, conversely, it cannot be introduced in the desired Hamiltonian if it is not present in the natural one. For example, an Ising Hamiltonian $H_I = \sigma_z \sigma_z$ is expanded as $H_I = (T_{00} + \sqrt{2}T_{20})/\sqrt{3}$, so that only the second part can be modulated. Conversely, the secular dipolar Hamiltonian is given by T_{20} , thus it cannot produce an Hamiltonian containing T_{00} (although it can be used to create the DQ-Hamiltonian, $\mathcal{H}_{DQ} = T_{22} + T_{2,-2}$). Group theory methods can be used to help solving Eq. (12) by reducing the number of conditions using symmetries. For

$\mathbb{1}$	$T_{00} = (\sigma_x^a \sigma_x^b + \sigma_y^a \sigma_y^b + \sigma_z^a \sigma_z^b)/\sqrt{3}$
$T_{10}^a = \sigma_z^a/2$	$T_{10}^b = \sigma_z^b/2$
$T_{11}^a = \sigma_+^a/\sqrt{2}$	$T_{11}^b = \sigma_-^b/\sqrt{2}$
$T_{11}^b = \sigma_+^b/\sqrt{2}$	$T_{1-1}^b = \sigma_-^b/\sqrt{2}$
$T_{11} = (\sigma_+^a \sigma_z^b - \sigma_z^a \sigma_+^b)/2$	$T_{1-1} = (\sigma_-^a \sigma_z^b - \sigma_z^a \sigma_-^b)/2$
$T_{10} = (\sigma_+^a \sigma_-^b - \sigma_-^a \sigma_+^b)/2$	$T_{20} = (2\sigma_z^a \sigma_z^b - \sigma_x^a \sigma_x^b - \sigma_y^a \sigma_y^b)/\sqrt{6}$
$T_{21} = (\sigma_+^a \sigma_z^b + \sigma_z^a \sigma_+^b)/2$	$T_{2-1} = (\sigma_-^a \sigma_z^b + \sigma_z^a \sigma_-^b)/2$
$T_{22} = \sigma_+^a \sigma_+^b/2$	$T_{2-2} = \sigma_-^a \sigma_-^b/2$

TABLE I. Spherical tensors for two spin-1/2 (a and b). σ_α are the usual Pauli operators.

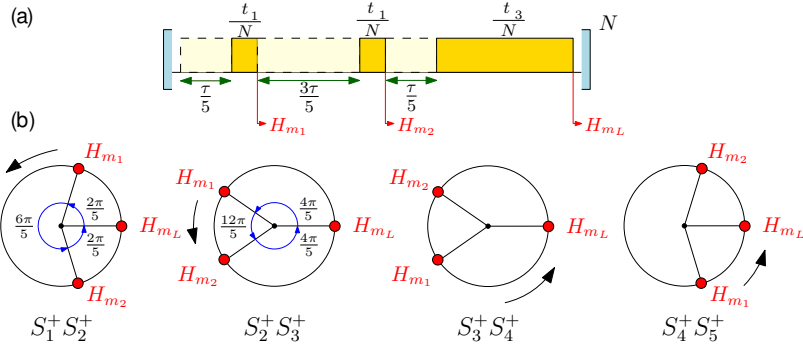


FIG. 7. Phasor representation of the recoupling sequence for $n = 5$. The phase acquired by the toggling frame Hamiltonians H_{m_j} after each mixing period in the sequence (a) is depicted on a unit circle for each of the NN terms $S_j^+ S_{(j+1)}^+$ in (b). The unit circle is traversed anti-clockwise from H_{m_1} to H_{m_L} . Mirror symmetry of the engineered couplings about the center of the chain is ensured since $\{S_1^+ S_2^+, S_4^+ S_5^+\}$ and $\{S_2^+ S_3^+, S_3^+ S_4^+\}$ have identical phasor representations. The DQ form of the average Hamiltonian is ensured by forcing that the phasors for each of the $S_j^+ S_{(j+1)}^+$ terms have reflection symmetry about 2π .

Chain Length	Mixing periods $\mathbf{t_m}$
4	$\{0, 0.067, 0.067, 0, 1.866\}$
5	$\{-0.201, -0.201, 2.1242\}$
6	$\{0.0987, 0.1559, 0.0987, 0.0987, 0.1559, -0.0987, 2.6882\}$
7	$\{-0.369, -0.0652, -0.0652, -0.369, 2.8806\}$
8	$\{-0.2169, 0.1340, 0.2169, 0.1182, 0.1182, 0.2169, 0.1340, -0.2169, 3.4957\}$
9	$\{-0.5269, -0.1298, -0.1298, -0.0316, -0.0316, -0.1298, -0.5269, 3.6492\}$
10	$\{-0.3433, 0.0995, 0.2116, 0.2524, 0.1316, 0.1316, 0.2524, 0.2116, 0.0995, -0.3433, 4.2963\}$
11	$\{-0.6801, -0.1920, -0.0666, -0.0183, -0.0183, -0.0666, -0.1920, -0.6801, 4.4231\}$

TABLE II. Mixing times $\mathbf{t_m}$ in units of $1/d$ (as used in Fig. 5 and Fig. 6). Note that $t_L \gg t_j$ for $j \neq L$.

example, the DQ Hamiltonian can be prepared from the secular dipolar Hamiltonian by using a simple sequence consisting of two time intervals, $t_1 = t_2/2$ with the Hamiltonian rotated by $R_2 = \frac{\pi}{2}|_y$ in second time period, to yield: $T_{2,0}t_1 + \left[\sqrt{\frac{3}{128}}(T_{2,2} + T_{2,-2}) - \frac{1}{2}T_{0,0}\right]t_2 \propto \mathcal{H}_{DQ}$. Symmetrized versions of this simple sequence are routinely used in NMR experiments [50].

Phasor representation of the engineering sequence

The filtered engineering sequence has an intuitive geometric visualization in terms of phasors, which demonstrates the symmetries involved in the QIT Hamiltonian and the subsequent choice of free evolution periods τ_z . Let us consider for example the 5-spin sequence (Fig. 7a), and the toggling frame Hamiltonians H_{m_j} during each mixing period. The phases acquired by the Hamiltonians are represented on a unit circle for each of the $S_j^+ S_{j+1}^+$ terms (Fig. 7b). The phasor representation makes clear the symmetries involved in the F_{ij} filter engineering. Since the ideal couplings d_j are mirror symmetric about the center of the chain, the construction of the filter $F_{j(j+1)}$ should match this symmetry. This can be ensured in two ways.

We could select a gradient centered around the mid-

dle spin in the chain. Then $\omega_j = -\omega_{n-j}$, and the set of equations in (4) reduces to only $n - 1$ equations (instead of $2(n - 1)$) if $t_k = t_{L-k}$ and $\mathcal{H}_m(\tau_k) = \mathcal{H}_m(\tau_{L-k})^\dagger$. This second condition further ensures that the first set of equations in Eq. (4) are satisfied (the condition is easily satisfied by setting $t_k^z = -t_{L-k}^z$ with $t_k^z = \tau_k - \tau_{k-1}$ and $t_1^z = \tau_1$). Thus we only have $\lceil(n - 1)/2\rceil$ equations to be satisfied and correspondingly only $\lceil(n - 1)/2\rceil$ mixing periods. Although solutions can be found with this scheme, only for $n = 4, 5$ all the times are real. For larger spin chains it is possible to find all real solutions for $L = \lceil(n - 1)/2\rceil + 2$ mixing periods, although the system of equations quickly becomes intractable.

A second strategy is to use a gradient with minimum at the first spin in the chain, $L = n - 2$ mixing periods (for n odd) and choose $\tau_j/\tau = 3/n$ for $j = (L + 1)/2$ and $\tau_j/\tau = 1/n$, and $t_j = t_{(L-j)}$. Moreover, since we want to retain the DQ form of the average Hamiltonian \bar{H} , the toggling frame Hamiltonians $H_m(\tau_k)$ and $H_m(\tau_{L-k})$ are such that their phasors have reflection symmetry about 2π for each $S_j^+ S_{j+1}^+$ term. This ensures that only the $(S_j^+ S_{j+1}^+ + S_j^- S_{j+1}^-) \cos[\tau\delta_{j(j+1)}]$ term survives, leading to an effective DQ form.

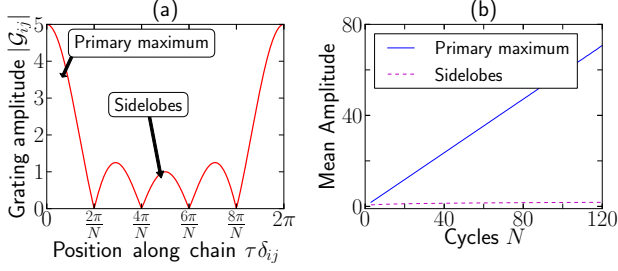


FIG. 8. (a) The amplitude of the dynamic Bragg grating, $|G_{ij}|$ for $N = 5$ cycles. There are $N - 1$ minima at $2j\pi/N$, and $N - 2$ secondary maxima (*sidelobes*). The width of the primary maximum is $2\pi/N$, and decreases with the number of cycles making the grating more selective. (b) Right panel characterizes the decoupling efficiency in terms of the mean amplitude of grating $|G_{ij}|$ in the primary maxima (i.e the range $[0, \pi/N] \cup [2(N-1)\pi/N, 2\pi/N]$), and the side lobes (the range $[\pi/N, 2(N-1)\pi/N]$). Increasing the number of cycles decreases the relative sideband power, and hence increases the grating selectivity.

Characterizing grating selectivity

Let us now characterize the selectivity of N -cycles of the Bragg grating $G_{ij} = \sum_{k=0}^{N-1} e^{ik\tau\delta_{ij}}$. Fig. 8(a) shows the grating amplitude $|G_{ij}|$ for $N = 5$ cycles. In general, the width of the primary maximum, $2\pi/N$, decreases with N and this increases the selectivity of the grating. Concurrently, the relative amplitude of the $N - 2$ sidelobes decreases with N . Specifically, consider Fig. 8(b), which compares the mean grating amplitude in the primary maxima i.e. in the range $[0, \pi/N] \cup [2(N-1)\pi/N, 2\pi/N]$, and the sidelobes in the range $[\pi/N, 2(N-1)\pi/N]$. From the properties of the Bragg grating, we find that the decoupling efficiency, characterized by the relative amplitude of the amplitude in the primary maxima with respect to the sidelobes, increases linearly with N .

Off resonance DQ excitation to construct U_z

In the main text, we assumed that the free evolution propagators U_z were constructed by employing a homonuclear decoupling sequence (for eg. WAHUA) during the τ_z intervals to refocus the internal Hamiltonian couplings, while leaving the action of the gradient. An alternate method is to use the DQ excitation sequence even during these periods, but shifting the offset frequency ω_0 far off-resonance. This is possible since the recoupling filter is periodic with a period $2m\pi$ thus we can shift ω_0 while retaining identical filter characteristics. Fig. 9 shows that an offset a few times larger than the coupling is sufficient to reach almost free evolution. Still, employing a decoupling sequence requires almost the same control requirements, and has the added ad-

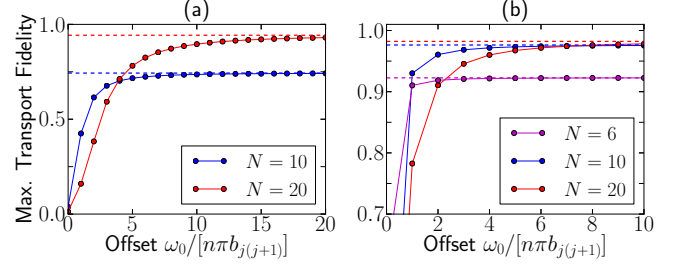


FIG. 9. A possible implementation of the U_z blocks is by shifting the offset frequency of the DQ excitation ω_0 to $m\pi b_{j(j+1)}$. Secular truncation ensures that even an offset by a few filter periods is sufficient to obtain fidelities (solid lines) comparable to when the U_z blocks are created by dipolar decoupling (dashed lines). We considered in (a) the network in Fig. 1 and in (b) a 9-spin chain with all couplings.

vantage of enhancing the net decoherence time of the system, allowing for transport in longer engineered spin chains.

- [1] S. Schirmer, in *Lagrangian and Hamiltonian Methods for Nonlinear Control 2006*, Lecture Notes in Control and Information Sciences, Vol. 366 (2007) pp. 293–304.
- [2] F. Verstraete, M. M. Wolf, and J. Ignacio Cirac, *Nat Phys* **5**, 633 (2009).
- [3] F. Ticozzi and L. Viola, *Automatica* **45**, 2002 (2009).
- [4] B. Kraus, H. P. Büchler, S. Diehl, A. Kantian, A. Micheli, and P. Zoller, *Phys. Rev. A* **78**, 042307 (2008).
- [5] D. P. DiVincenzo, D. Bacon, J. Kempe, G. Burkard, and K. B. Whaley, *Nature* **408**, 339 (2000).
- [6] P. Cappellaro and M. D. Lukin, *Phys. Rev. A* **80**, 032311 (2009).
- [7] A. Ajoy, G. A. Álvarez, and D. Suter, *Phys. Rev. A* **83**, 032303 (2011).
- [8] M. J. Biercuk, A. C. Doherty, and H. Uys, *J. of Phys. B* **44**, 154002 (2011).
- [9] J. I. Cirac and P. Zoller, *Nat Phys* **8**, 264 (2012).
- [10] R. P. Feynman, *Internat. J. Theoret. Phys.* **21**, 467 (1982).
- [11] A. Ajoy, R. K. Rao, A. Kumar, and P. Rungta, *Phys. Rev. A* **85**, 030303 (2012).
- [12] R. Blatt and C. F. Roos, *Nat Phys* **8**, 277 (2012).
- [13] S. Lloyd, *Science* **273**, 1073 (1996).
- [14] M. Suzuki, *Phys. Lett. A* **146**, 319 (1990).
- [15] W. S. Bakr, J. I. Gillen, A. Peng, S. Folling, and M. Greiner, *Nature* **462**, 74 (2009).
- [16] P. E. S. Smith, G. Bensky, G. A. Álvarez, G. Kurizki, and L. Frydman, *Proc. Nat. Acad. Sc.* **109**, 5958 (2012).
- [17] S. Bose, *Phys. Rev. Lett.* **91**, 207901 (2003).
- [18] M. Christandl, N. Datta, A. Ekert, and A. J. Landahl, *Phys. Rev. Lett.* **92**, 187902 (2004).
- [19] J. Baum, M. Munowitz, A. N. Garroway, and A. Pines, *J. Chem. Phys.* **83**, 2015 (1985).
- [20] D. Suter, S. Liu, J. Baum, and A. Pines, *Chem. Phys.* **114**, 103 (1987).

- [21] N. Y. Yao, L. Jiang, A. V. Gorshkov, Z.-X. Gong, A. Zhai, L.-M. Duan, and M. D. Lukin, *Phys. Rev. Lett.* **106**, 040505 (2011).
- [22] P. Cappellaro, L. Viola, and C. Ramanathan, *Phys. Rev. A* **83**, 032304 (2011).
- [23] A. Ajoy and P. Cappellaro, *Phys. Rev. A* **85**, 042305 (2012).
- [24] J. Fitzsimons and J. Twamley, *Phys. Rev. Lett.* **97**, 090502 (2006).
- [25] C. DiFranco, M. Paternostro, and M. S. Kim, *Phys. Rev. Lett.* **101**, 230502 (2008).
- [26] M. Markiewicz and M. Wiesniak, *Phys. Rev. A* **79**, 054304 (2009).
- [27] C. Albanese, M. Christandl, N. Datta, and A. Ekert, *Phys. Rev. Lett.* **93**, 230502 (2004).
- [28] F. W. Strauch and C. J. Williams, *Phys. Rev. B* **78**, 094516 (2008).
- [29] A. Kay, *Phys. Rev. A* **73**, 032306 (2006).
- [30] J. Waugh, L. Huber, and U. Haeberlen, *Phys. Rev. Lett.* **20**, 180 (1968).
- [31] U. Haeberlen, *High Resolution NMR in Solids: Selective Averaging* (Academic Press Inc., New York, 1976).
- [32] G. S. Boutis, P. Cappellaro, H. Cho, C. Ramanathan, and D. G. Cory, *J. Mag. Res.* **161**, 132 (2003).
- [33] G. A. Álvarez, A. Ajoy, X. Peng, and D. Suter, *Phys. Rev. A* **82**, 042306 (2010).
- [34] G. A. Álvarez, M. Mishkovsky, E. P. Danieli, P. R. Levstein, H. M. Pastawski, and L. Frydman, *Phys. Rev. A* **81**, 060302 (2010).
- [35] E. Vinogradov, P. Madhu, and S. Vega, *Chem. Phys. Lett.* **314**, 443 (1999).
- [36] P. Karbach and J. Stolze, *Phys. Rev. A* **72**, 030301 (2005).
- [37] M. H. Levitt, *J. Chem. Phys.* **128**, 052205 (2008).
- [38] A. Wojcik, T. Luczak, P. Kurzynski, A. Grudka, T. Gdala, and M. Bednarska, *Phys. Rev. A* **72**, 034303 (2005).
- [39] G. Gualdi, V. Kostak, I. Marzoli, and P. Tombesi, *Phys. Rev. A* **78**, 022325 (2008).
- [40] A. Ajoy and P. Cappellaro, “Perfect quantum state transport in arbitrary spin networks,” Unpublished.
- [41] S. Oishi and T. Kamiya, *Nippon Kagaku Kaishi* **9**, 800 (1994).
- [42] A. Sur, D. Jasnow, and I. J. Lowe, *Phys. Rev. B* **12**, 3845 (1975).
- [43] P. Cappellaro, C. Ramanathan, and D. G. Cory, *Phys. Rev. Lett.* **99**, 250506 (2007).
- [44] G. Kaur and P. Cappellaro, *New J. Phys.* **14**, 083005 (2012).
- [45] W. Zhang and D. G. Cory, *Phys. Rev. Lett.* **80**, 1324 (1998).
- [46] Y. Rumala, BS thesis (CUNY, New York) (2006).
- [47] D. Rugar, R. Budakian, H. J. Mamin, and B. W. Chui, *Nature* **430**, 329 (2004).
- [48] H. J. Mamin, C. T. Rettner, M. H. Sherwood, L. Gao, and D. Rugar, *App. Phys. Lett.* **100**, 013102 (2012).
- [49] W. Zhang, P. Cappellaro, N. Antler, B. Pepper, D. G. Cory, V. V. Dobrovitski, C. Ramanathan, and L. Viola, *Phys. Rev. A* **80**, 052323 (2009).
- [50] C. Ramanathan, H. Cho, P. Cappellaro, G. S. Boutis, and D. G. Cory, *Chem. Phys. Lett.* **369**, 311 (2003).